Earth and Planetary Science Letters 496 (2018) 120–131

Contents lists available at ScienceDirect

Earth and Planetary Science Letters

www.elsevier.com/locate/epsl

Early Miocene birth of modern Pearl River recorded low-relief, high-elevation surface formation of SE Tibetan Plateau

Licheng Cao [a], Lei Shao [a,*], Peijun Qiao [a], Zhigang Zhao [b], Douwe J.J. van Hinsbergen [c]

[a] State Key Laboratory of Marine Geology, Tongji University, Shanghai 200092, China
[b] Research Institute of China National Offshore Oil Corporation, Beijing 100027, China
[c] Department of Earth Sciences, Utrecht University, Heidelberglaan 2, 3584 CS Utrecht, Netherlands

ARTICLE INFO

Article history:
Received 21 December 2017
Received in revised form 3 May 2018
Accepted 21 May 2018
Available online xxxx
Editor: A. Yin

Keywords:
provenance
zircon U–Pb geochronology
South China Sea
Pearl River
Tibetan Plateau
topography

ABSTRACT

Understanding the paradoxical presence of extensive low-relief surfaces perched above deep valleys in SE Tibet is a long-standing challenge. Its origin, based on topographic analysis, has been explained traditionally by incision of a regional relict landscape or, more recently, by in situ formation in response to drainage area loss feedback. Here we apply a qualitative and quantitative source-to-sink approach to test whether either of the two mechanisms may apply by establishing potential links among detrital zircon provenance of the Oligocene–Miocene Pearl River Mouth Basin, drainage evolution of the Pearl River, and low-relief, high-elevation surface formation in the SE Tibetan Plateau margin. Our zircon record, combined with previous geochemical records from the northern South China Sea, confirms a significant Late Oligocene provenance shift, represented by an intensive addition of Proterozoic zircons and a gradual negative excursion in Nd isotopes. We interpret this provenance shift as a response to a progressive drainage expansion of the Pearl River, evolving from relatively small rivers confined to coastal South China in the Early Oligocene to a near-modern continental-scale drainage configuration in the Early Miocene, which may be correlated with an earlier surface uplift of SE Tibet than previously thought. This westward expansion process of the Pearl River favors the envisaged drainage evolution of the relict landscape model over that of the drainage area loss feedback model, suggesting that the Middle–Late Cenozoic low-relief, high-elevation surface formation in SE Tibet may be readily interpreted as preserving past tectonic and environmental conditions.

1. Introduction

Plate tectonics generates short-wavelength deformation at plate margins, where rock uplift is often countered by fluvial and glacial incisions and coupled mountain collapse, resulting in a commonly observed elevated, rugged topography. A notable exception to this pattern exists in the SE Tibetan Plateau where extensive areas of low topographic relief are perched high in craggy mountain ranges (Fig. 1), and its origin has long been puzzling. The conventional explanation posits that these surfaces are remnants of a formerly continuous, if complex, elevated, low-relief landscape that is undergoing an initial stage of fluvial dissection, although whether the purported relict landscape formed near sea level or at high elevation is debated (Fig. 2a; Clark et al., 2006; Liu-Zeng et al., 2008). More recently and in contrast, there has been an emerging focus on the previously underappreciated role of drainage dynamics in shaping landscapes (Willett et al., 2014). In this light, Yang et al. (2015) argued that the feedback process following local drainage area loss, by way of divide migration and river capture, is capable of leading to an in situ, self-sustained formation of relief reduction and surface uplift (Fig. 2b). The two mechanisms may be complementary, but it is important to determine which one is dominant in tectonically active regions like SE Tibet. Unfortunately, most of these inferences are still observationally and theoretically rooted in morphometric analysis that embeds many simplifying assumptions (Robl et al., 2017) in terms of boundary conditions and variables (e.g., precipitation and sediment load) to describe natural landscapes. For this reason, the interpretation of topographic metrics (e.g., slope-elevation distributions and χ-transformed channel profiles) and the proposed diagnostic criteria of landscape characteristics (e.g., variability in knickpoint elevations and co-planarity of low-relief surfaces) remain controversial (Yang et al., 2015; Whipple et al., 2017). Relict and in situ-generated low-relief, high-elevation landscapes thus seem not to be readily distinguishable by morphometric methods alone.

* Corresponding author at: State Key Laboratory of Marine Geology, Tongji University, 1239 Siping Road, Shanghai 200092, China.
E-mail address: lshao@tongji.edu.cn (L. Shao).

https://doi.org/10.1016/j.epsl.2018.05.039
0012-821X/

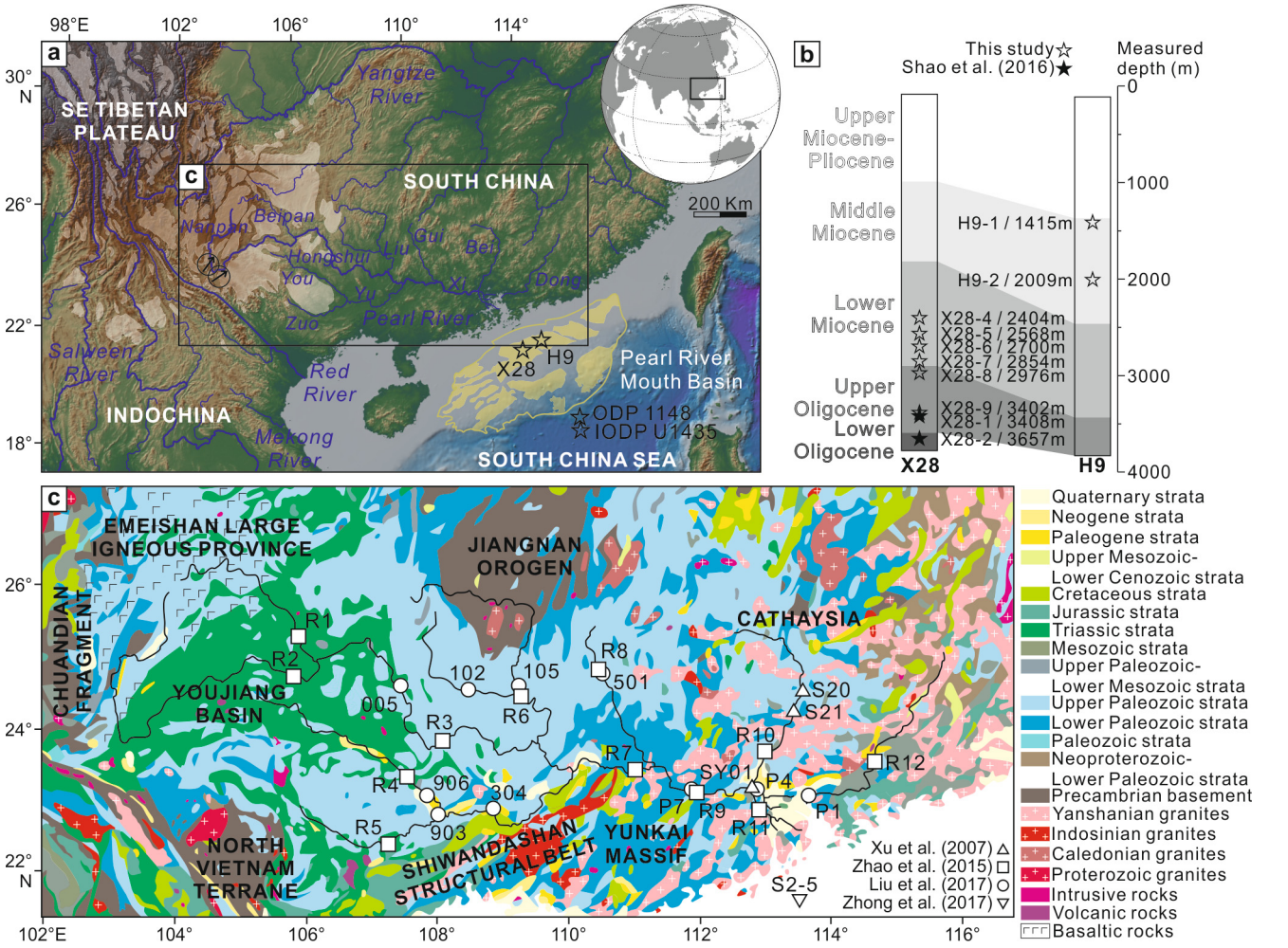

Fig. 1. (a) Topographic map of the study area showing large rivers flowing from the SE Tibetan Plateau to the South China–Indochina margin and the localities of studied commercial boreholes (X28 and H9) drilled in the Pearl River Mouth Basin. The previous ODP Site 1148 and IODP Site U1435 drilled close to the continental-oceanic boundary are also shown. White and yellow shaded areas represent low-relief, high-elevation surfaces in the SE Tibetan Plateau (Clark et al., 2006) and main depressions in the Pearl River Mouth Basin, respectively. Two black arrows between the Nanpan River and Red River trunk mark the northeastward paleocurrent directions of the Eocene fluvial deposits (Wissink et al., 2016). (b) Simplified stratigraphic columns of boreholes X28 and H9 showing the positions of Oligocene to Middle Miocene samples analyzed in this study and by Shao et al. (2016). (c) Geological map of the Pearl River drainage basin displaying the locations of previous modern samples collected from river courses and near estuary (see Table S1 for compiled data and references). (For interpretation of the colors in this figure, the reader is referred to the web version of this article.)

The prolonged evolution of fluvial landscapes under the complex interplay of exogenic and endogenic factors may be archived in deep-time sediment sinks (Allen, 2008). It may thus be possible to trace the origin of low-relief, high-elevation topography in SE Tibet through the provenance data acquired from sedimentary basins where Tibetan rivers deposit their sediment load. The most promising river to host such topographic information for SE Tibet may be the Pearl River, China's second largest river. The Pearl River trunk stream, Xi River, presently originates from the low-relief plateau margin of SE Yunnan and confluences with another two main tributaries (Bei River and Dong River) at the river mouth emptying into the South China Sea (Fig. 1a). The understanding regarding the Pearl River drainage evolution has initially benefited from provenance studies of Ocean Drilling Program (ODP) Site 1148 (Fig. 1a) of which a negative ~2 εNd unit excursion around the Oligocene–Miocene boundary has been interpreted to be associated with an expansion of the Pearl River drainage network from the South China margin to the continental interior (Clift et al., 2002). This interpretation is also supported by a growing body of provenance data from commercial boreholes in the Pearl River Mouth Basin (e.g., Shao et al., 2008; 2015) and International Ocean Discovery Program (IODP) Site U1435 near the continental-oceanic boundary (Fig. 1a; Liu et al., 2017; Shao et al., 2017). However, the extent and evolution of the paleo-Pearl River drainage basin are still far from being clearly outlined, mainly due to incomplete or ambiguous characterization of source areas, inferior discriminatory power of traditional provenance proxies, as well as additional complexity from intrabasinal source supplies (Shao et al., 2016).

In this study, we employ detrital zircon U–Pb geochronology on Oligocene–Middle Miocene strata from the northern Pearl River Mouth Basin (Fig. 1b). This source-to-sink system is chosen for several reasons. First, identifying the evolution of such a large fluvial system on land is challenging due to difficulties in facies interpretation and scarcity of preserved fluvial deposits whereas the river mouth basin contains a continuous and datable sedimentary archive. Second, in contrast to other adjacent large rivers draining SE Tibet (e.g., Yangtze River), the lithological distribution within the Pearl River drainage basin is relatively simple (Fig. 1c), and the obtained provenance signatures may be easier correlated with specific source areas. Third, compared to traditional provenance proxies like whole-rock geochemistry, zircon U–Pb geochronology is less sensitive to the effects of hydraulic sorting and chemical dissolution, and has been shown to be more powerful in exquisitely distinguishing different source terranes. Fourth, there is already a large zircon age database derived from modern sediments and outcropping bedrocks in the drainage basin, and re-

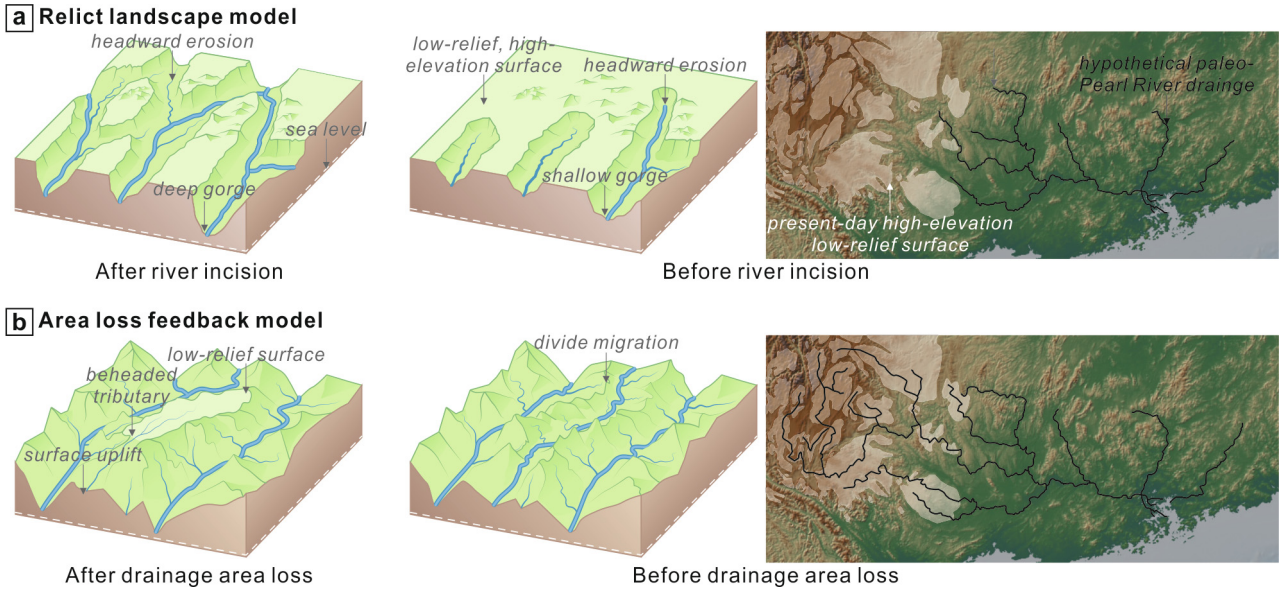

Fig. 2. Schematic models illustrating formation mechanisms of low-relief, high-elevation surfaces in the SE Tibetan Plateau and corresponding hypothetical drainage evolution of the paleo-Pearl River. (a) The relict landscape model (Clark et al., 2006; Liu-Zeng et al., 2008): the low-relief, high-elevation surface patches together constitute a formerly continuous, regional-scale landscape that has been later reshaped by the headward-propagating incision of rivers including the upper paleo-Pearl River. (b) The area loss feedback model (Yang et al., 2015): the present-day low-relief areas in SE Tibet may be initially drained by external drainages of the paleo-Pearl River. Subsequent drainage area loss of these catchments via divide migration resulted in in situ surface uplift and relief reduction, along with intensified incision in surrounding capturing rivers that are aggressively advancing into its current drainage distribution of the Pearl River.

cent advances in sediment mixture modeling (Sundell and Saylor, 2017) allow a quantitative determination of relative contributions from each source area. In comparison to previous morphometric, thermochronometric, and paleoaltimetric analyses centered on the headwater region, the newly acquired provenance record is expected to present a holistic view of drainage evolution, which we use to evaluate whether the Pearl River may provide new insights into the low-relief, high-elevation surface formation of the SE Tibetan Plateau.

2. Geological setting

2.1. SE Tibet

The uplift of SE Tibet has been associated with the India-Asia collision and convergence since the Early Cenozoic (Yin and Harrison, 2000; Li et al., 2017), and explained as a consequence of either rigid block extrusion (e.g., Tapponnier et al., 2001), or internal deformation including ductile crustal flow in restricted zones and vertically coherent lithospheric deformation (e.g., Clark and Royden, 2000; Wang et al., 2008), or a combination thereof (e.g., Liu et al., 2014). The uplift history of SE Tibet, despite decades of research, proves difficult to unequivocally reconstruct. Rapid exhumation starting around 10–15 Ma, documented by low-temperature thermochronology in river gorges dissecting SE Tibet, is often inferred to mark the onset of fluvial incision and plateau growth (Clark et al., 2005; Ouimet et al., 2010). The growing recognition of Oligocene–Early Miocene rapid cooling episodes also hints at the possibility of earlier periods of exhumation (e.g., Wang et al., 2012; Shen et al., 2016; Wang et al., 2016). However, there is likely a considerable time lag between tectonic exhumation and surface uplift, and in view of changing climatic conditions, river incision may not be a reliable proxy to date the inception of regional topographic rise (England and Molnar, 1990). Recent stable isotope paleoaltimetry results suggested that the elevated Tibetan Plateau already expanded southeastward to NW Yunnan in the Eocene, and the plateau margin of SE Yunnan likely attained its near-modern elevation of 1.6 km no later than the Middle Miocene (Hoke et al., 2014; Li et al., 2015). These isotope-based paleoelevation estimates, despite large methodological uncertainties and low spatial and temporal resolution, may be still reliable (Li and Garzione, 2017).

2.2. Pearl River Mouth Basin

Prolonged extension along the South China margin since the Late Cretaceous resulted in the formation of a series of the Paleogene rift basins in southeastern South China and the northern South China Sea (Morley, 2016). The earliest rifting in the northern part of the Pearl River Mouth Basin, manifested by the development of fault-bounded half-grabens and asymmetric grabens, was initiated during the Late Paleocene (Fig. 3). The overlying Paleocene–Eocene syn-rift sequences are generally characterized by fluvial and lacustrine facies with occasional volcaniclastic intercalations (Zhao et al., 2009; Wang et al., 2017). Following the onset of the South China Sea spreading at ~33 Ma (Li et al., 2014), the Oligocene deposition in the Pearl River Mouth Basin was dominated by sandstones of transitional facies. Extensive seismic and borehole data acquired from previous commercial and scientific drilling expeditions on the northern South China Sea margin have revealed that a significant unconformity spanning 2.5–3 Ma marks the initiation of the post-rift stage after the Late Oligocene (Pang et al., 2009). During the Neogene, the Pearl River Mouth Basin was dominated by a carbonate platform-continental shelf-deltaic environment (Fig. 3).

3. Provenance hypotheses

3.1. Hypothetical drainage evolution

The possible patterns of propagation of topographic signals and drainage evolution of the Pearl River in the context of two end-member mechanisms of low-relief upland formation are envisaged as follows to assess the distinguishability of corresponding provenance scenarios and to facilitate the subsequent definition of potential source areas.

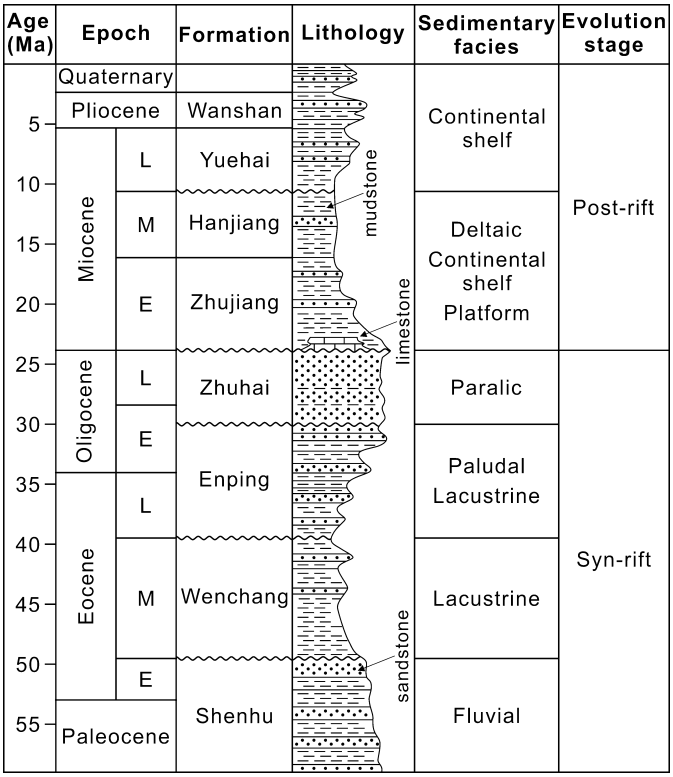

Fig. 3. Schematic stratigraphic column of the northern Pearl River Mouth Basin (modified from Zhao et al., 2009).

In the relict landscape model, the low-relief surfaces in SE Tibet would form as a slowly eroding peneplain near sea level in the Early Cenozoic before the Late Cenozoic regional-scale uplift (Clark et al., 2006). Alternatively, Liu-Zeng et al. (2008) proposed that the topographic flatness of this region may have been produced in a similar manner to that of central Tibet, i.e., by diachronous beveling at high elevation. Either way, the relict landscape model generally assumes that the formation of low-relief surfaces precedes river dissection, which in the paleo-Pearl River case represents a westward expansion of its drainage area into the plateau margin by headwater erosion (Fig. 2a).

The recent area loss feedback model (Yang et al., 2015) suggests that the initial state of low-relief surfaces tends to mountainous and externally drained where subsequent drainage area loss in response to external forcings may lead to a cascading decrease in water discharge and sediment supply, along with in situ relief reduction and surface uplift. By contrast, capturing rivers bounding these continuously modified victim drainage basins are aggressively advancing into their present-day trunk drainage networks (Fig. 2b). This feedback in the paleo-Pearl River case would likely be expressed in terms of progressive divide migration rather than punctuated river capture. On the one hand, the long-debated, regional-scale drainage reorganization between Yangtze and Red rivers almost never involves an intervention of change in the paleo-Pearl River drainage area (e.g., Clift et al., 2006; Zheng et al., 2013). Recent paleocurrent measurements of fluvial conglomerates from between the Nanpan River and Red River trunk also supported that the divide between the Pearl and Red river catchments already existed since the Eocene (Fig. 1a; Wissink et al., 2016). On the other hand, although the northwesternmost South China Sea has been sometimes supposed to be an earlier sink of rivers flowing from the plateau margin (e.g., Hoang et al., 2009), the possibility of this sediment routing system is limited by the pre-Cenozoic Shiwandashan Structural Belt acting as a barrier (Fig. 1c). Thus, during the function of area loss feedback the plateau margin is expected to be continuously drained by the paleo-Pearl River, and prior to the initiation of this feedback the headwater paleo-Pearl River may have rather drained areas of the Emeishan region and Chuandian Fragment than presently observed (Figs. 1 and 2b).

Taken together, the above two models assume an overall expansion or contraction of the Pearl River drainage network, which may be readily distinguished by provenance data from the Pearl River Mouth Basin. Meanwhile, both models require tectonic perturbations to cause regional uplift of SE Tibet concurrent with or prior to either the initial river incision (Clark et al., 2006; Liu-Zeng et al., 2008) or the onset of area loss feedback (Yang et al., 2015). Thus, the expected provenance shift in response to drainage evolution of the Pearl River may provide a minimum estimate of the timing of uplift in headwater areas.

3.2. Defining potential sources

Unlike previous provenance studies of the South China Sea region that usually defined the different source areas on a plate or subplate scale, this study investigates published zircon age data from the Pearl River drainage basin (Fig. 4; Table S1) to consider lithological heterogeneity and structural complexity within South China. Age data of zircons from modern drainage sediments are preferred to those from bedrocks because the former provide a time-averaged estimate of magmatic events present at a hundreds-of-kilometers scale, whereas the latter tends to be biased by sampling strategy, preservation potential, and exposure. Meanwhile, we mainly focus on samples from upper reaches and major tributaries to avoid the downstream mixture of zircon grains. The traditional visual inter-sample comparison of kernel density estimation (KDE) spectra and histograms is further aided by the dimension-reducing technique multidimensional scaling (MDS). The MDS dissimilarity is calculated as the cross-correlation coefficient for KDE spectra and the Kolmogorov–Smirnov (K–S) test statistic for cumulative distribution functions (Saylor and Sundell, 2016), and both two metrics yield a largely consistent pattern of relative similarities among most samples (Fig. 5). By grouping the samples with similar age signatures and linking them to regional lithological distributions and magmatic events, seven diagnostic potential provenances are accordingly defined (Fig. 6). Noteworthy is that these source areas are generally in accordance with the distribution of major tributaries.

The Bei and Dong rivers drain eastern Cathaysia where outcropping bedrocks are dominated by the Yanshanian (70–190 Ma) granites (Fig. 1c). The Dong River Provenance (samples P1 and R12) is characterized by two strong age peaks at ca. 160 Ma and ca. 450 Ma as well as a population of Triassic and Cretaceous ages (Fig. 6). Although the upstream Bei River sample (S20), due to insufficient zircon analyses, is separate from the downstream samples (S21 and R10) in the MDS maps (Figs. 4 and 5), the overall age signature of the Bei River Provenance differs from that of the Dong River Provenance with fewer Caledonian (400–500 Ma) and late Yanshanian populations (Fig. 6).

As tributaries to the middle Xi River, the Liu and Gui rivers are derived from the western segment of the Jiangnan Orogen that is a Neoproterozoic accretionary orogenic belt associated with the Yangtze–Cathaysia collision (Lehrmann et al., 2015) and downstream flow through the Paleozoic terranes (Fig. 1c). Samples R6, 102, and 105 are clearly grouped in the MDS plots (Fig. 5), representing the Liu River Provenance characteristic of a strong age peak at ca. 790 Ma (Fig. 6). By contrast, the Gui River Provenance (samples R8 and 501) displays a dominant Early Neoproterozoic cluster peaking at ca. 970 Ma as well as a percentage of Paleo–Mesoproterozoic and Late Neoproterozoic–Early Paleozoic ages (Fig. 6).

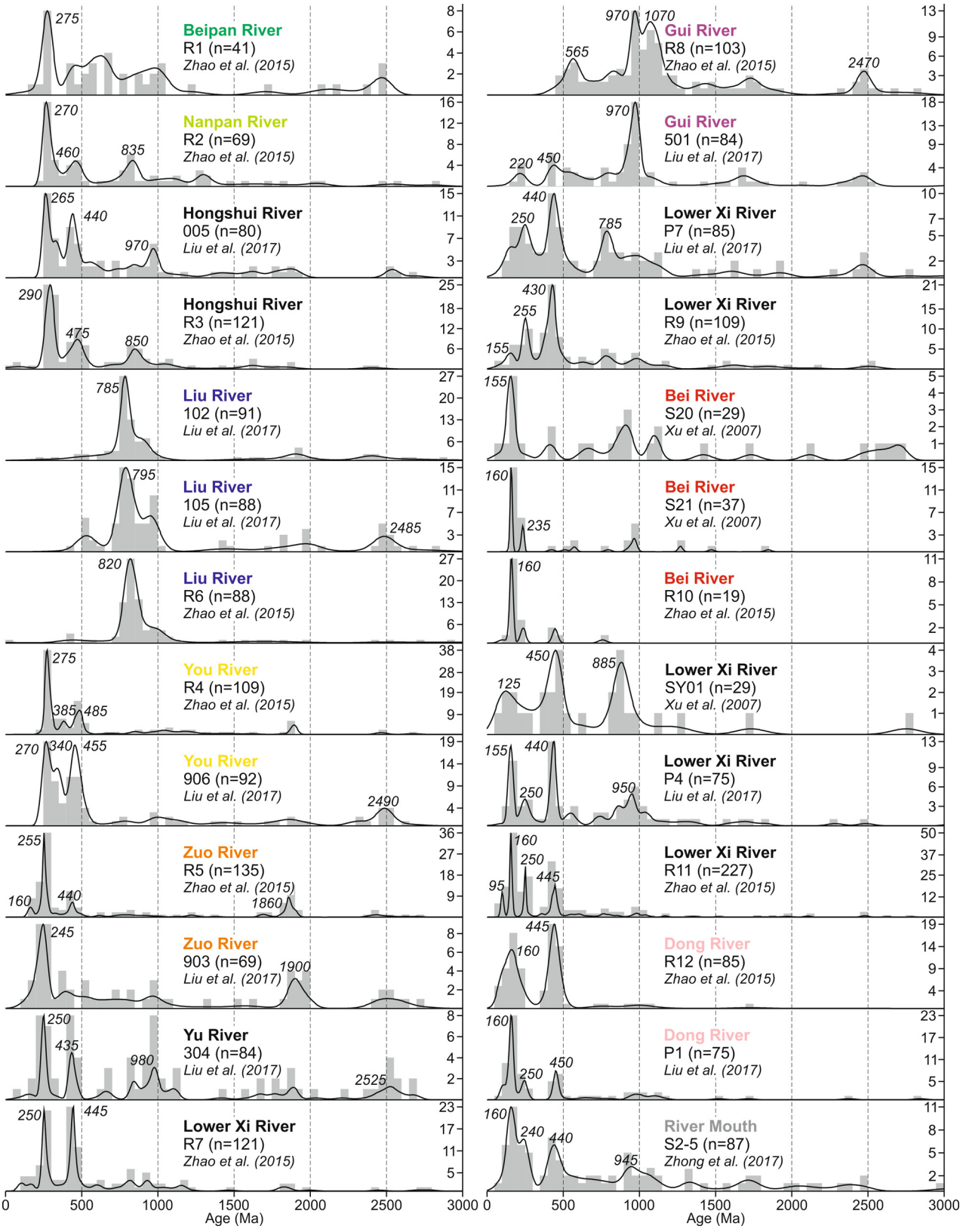

Fig. 4. Compilation of published detrital zircon U–Pb ages of modern sediments from the Pearl River drainage basin and near the river mouth, shown as histograms and kernel density estimation (KDE) spectra. *n*—number of concordant analyses. See Fig. 1c for the localities of tributary and estuary samples (colored) and confluence samples (black). Compiled data and references are given in Table S1. (For interpretation of the colors in this figure, the reader is referred to the web version of this article.)

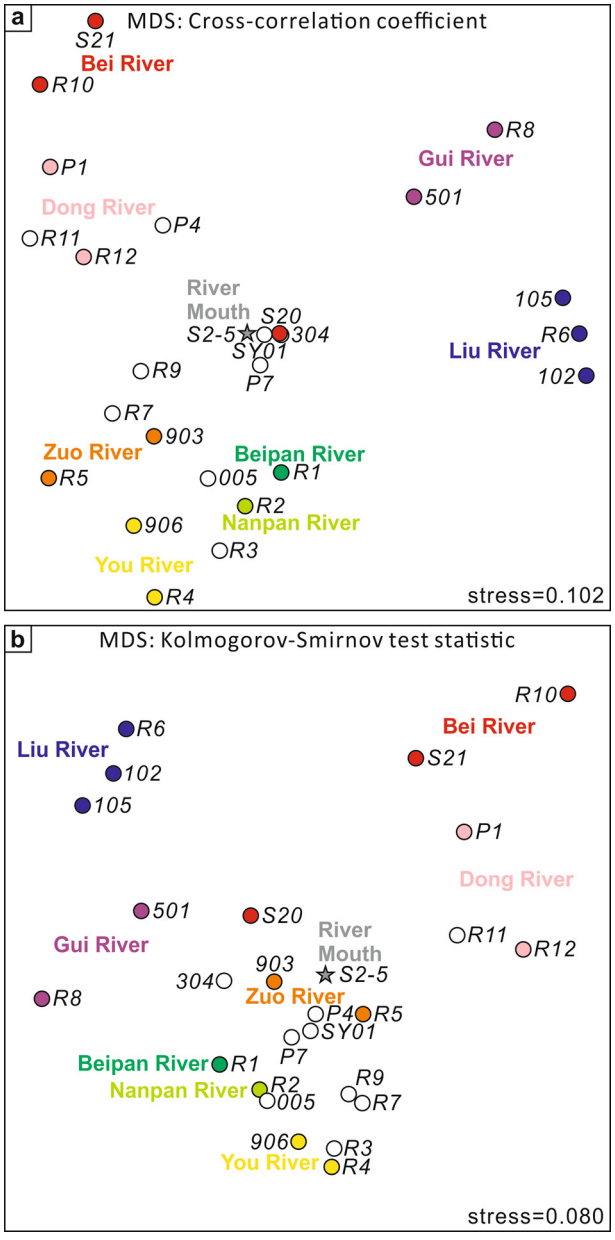

Fig. 5. Nonmetric multidimensional scaling (MDS) maps for compiled detrital zircon U–Pb ages of modern sediments from the Pearl River drainage basin and near the river mouth, with dissimilarity calculated as (a) cross-correlation coefficient and (b) Kolmogorov–Smirnov (K–S) test statistic, respectively. Samples are represented as a point with greater distances between two points indicating greater dissimilarity between the two age distributions. The stress values of MDS statistics indicate a good to fair goodness-of-fit. Tributary and estuary samples are color-coded as marked in Fig. 4. (For interpretation of the colors in this figure, the reader is referred to the web version of this article.)

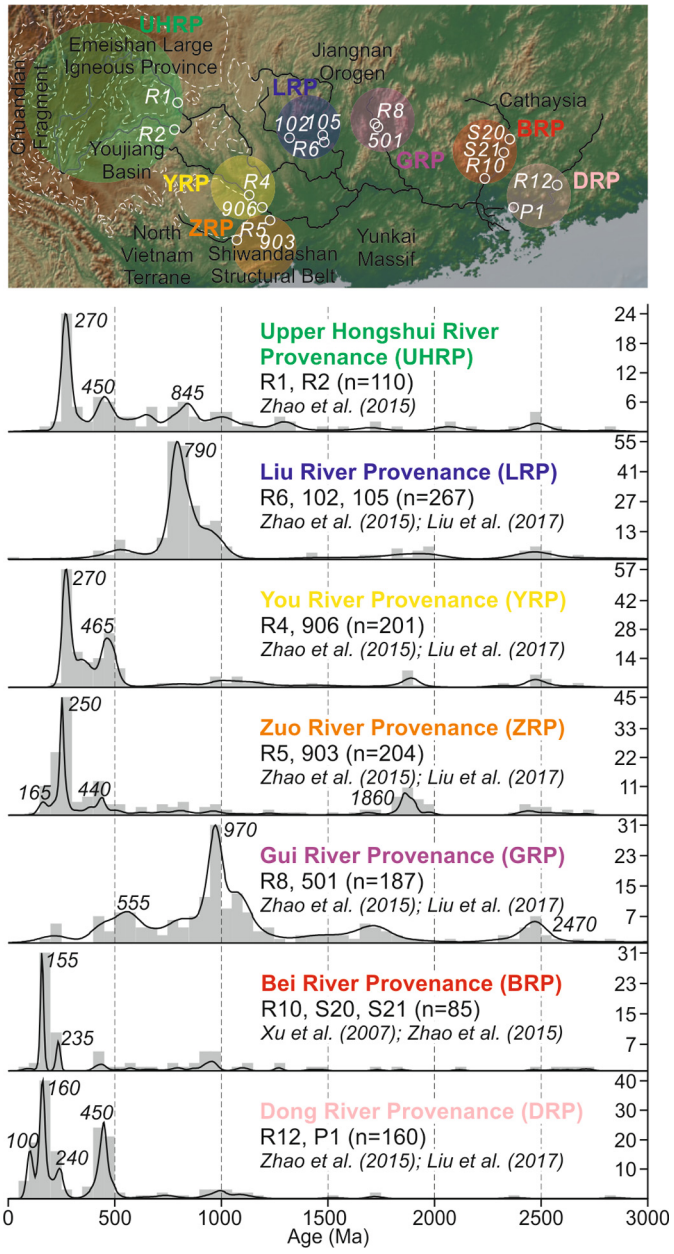

Fig. 6. Topographic map schematically showing seven defined potential provenances areas (colored circles) along with their zircon age signatures shown as kernel density estimation (KDE) spectra and histograms. The present-day low-relief, high-elevation surfaces in SE Tibet (dashed lines; Clark et al., 2006) and drainage sediment samples used for compilation of published zircon U–Pb ages are also marked. *n*—number of concordant analyses.

The upper Yu River, consisting of You River and Zuo River, drains the SE Youjiang Basin (Nanpanjiang Basin) that is mainly filled by Upper Paleozoic carbonates and Triassic deep marine turbidites (Fig. 1c). Zircons from the You River Provenance (samples R4 and 906) are generally dated with Caledonian and Hercynian (250–350 Ma) ages peaking at ca. 465 Ma and ca. 270 Ma, respectively (Fig. 6). By contrast, samples R5 and 903 from the adjacent Zuo River Provenance show fewer Caledonian ages and a higher percentage of Paleoproterozoic, Indosinian (200–250 Ma), and early Yanshanian ages (Fig. 6); the distinct presence of these Mesozoic zircons can be well correlated with the extensive Jurassic–Cretaceous strata and Indosinian granites outcropping along the Shiwandashan Structural Belt to the south (Fig. 1c).

The Beipan and Nanpan rivers, constituting the headwater Xi River, drain the NW Youjiang Basin (Fig. 1c), and their age distributions contrast with that of the You River with the existence of more Proterozoic populations (Fig. 4). Farther west and north, the Emeishan Large Igneous Province and Chuandian Fragment, albeit lithologically and geochronologically distinguishable (Fig. 1c), are not defined as individual provenances in Fig. 6, because for a prolonged geologic history they have been topographic highs supplying siliciclastic sediments to western Yangtze (Yang et al., 2014; Lehrmann et al., 2015) and their age signatures tend to be masked by that of bedrocks in the NW Youjiang Basin. Instead, we include the age data of samples R1 and R2 to generally characterize the Upper Hongshui River Provenance (Fig. 6).

Although age signature of bedrocks exposed along the lower Xi River cannot be identified using our strategy for data selection and subdivision of provenance areas, the comparable lithological distribution between the lower Xi River trunk and eastern Cathaysia (Fig. 1c) suggests that provenance contribution from the lower Xi River may be indirectly reflected by a combination of Bei River Provenance and Dong River Provenance (Fig. 6). This inference is supported by the local provenance signature observed in sample R11 near the Xi river mouth, where the zircon age distribution pattern is clearly different from that of other samples (P7, R9, SY01, and P4) from the lower Xi River but similar to that of the Dong River samples (Figs. 4 and 5). For this reason, the Yunkai Massif, bordering the lower Xi River catchment, is not defined as an individual provenance.

4. Samples and methods

8 sandstone samples from boreholes X28 and H9 in the northern Pearl River Mouth Basin were collected (Fig. 1). Their stratigraphic ages were based on unpublished seismic and paleontological data from China National Offshore Oil Corporation (CNOOC). Due to the relatively limited resolution and precision of age models in commercial boreholes, the studied samples were assigned to four stratigraphic intervals, i.e., Lower Oligocene, Upper Oligocene, Lower Miocene, and Middle Miocene.

U–Pb dating was performed by laser ablation-inductively coupled plasma-mass spectroscopy (LA-ICP-MS) in the State Key Laboratory of Marine Geology of Tongji University, China. The instrumentation comprises a Thermo Elemental X-Series ICP-MS coupled to a New Wave 213 nm laser ablation system, and detailed analytical procedures are described by Shao et al. (2016). Cathodoluminescence images were used to locate analytical spots (20–30 μm) in zircon oscillatory zoning. U–Th–Pb isotopic ratios were calculated using ICPMSDataCal (Liu et al., 2009) followed by the common Pb correction method of (Andersen, 2002). The accepted ages were selected from a subset of both $\leq$10% discordance and $\leq$10% uncertainty (1σ), wherein the $^{206}Pb/^{238}U$ and $^{207}Pb/^{206}Pb$ ages were adopted for zircons younger and older than 1000 Ma, respectively. Age distributions are visualized as histograms (bin width = 50 Ma) and KDE spectra (adaptive bandwidth $\leq$30 Ma).

5. Results

The U–Pb age results of eight analyzed samples (Table S2) along with previous data of two Oligocene samples from borehole X28 (Shao et al., 2016) are graphically shown in Fig. S1, which shows a certain degree of intra-stratal variation in zircon age signatures especially in the Upper Oligocene and Lower Miocene strata. Considering that within each stratum the zircon age distribution patterns of the stratigraphically highest and lowest samples are largely comparable, and that the intra-stratal variations are mostly expressed by the different percentage rather than the appearance or disappearance of major age clusters, we tentatively grouped the samples according to their corresponding stratigraphic positions (Fig. 7). Published age data of Paleogene strata from several commercial boreholes further south are not included here to avoid the potential complexity of intrabasinal provenances (Shao et al., 2016) as well as the significant bias of inter-borehole comparison induced by a limited number of analyzed zircons (typically around 20–30) in each sample (e.g., Wang et al., 2017).

Due to strong anthropogenic disturbances since the Late Holocene, the modern Pearl River has been considered not representative of a modern analog for understanding controls on erosion and weathering in the geologic past (e.g., Hu et al., 2013); however, zircon grains are generally transported as bedload and their residence times in continental-scale drainage basins have been estimated to

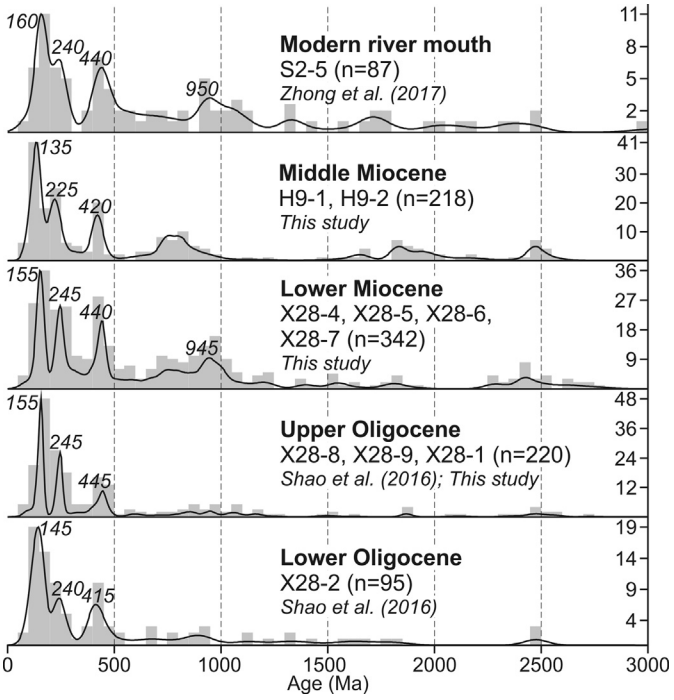

Fig. 7. Comparison of zircon U–Pb ages from Oligocene–Middle Miocene strata of boreholes X28 and H9 in the northern Pearl River Mouth Basin as well as modern coastal sediments near the river mouth. *n*—number of concordant analyses.

be mostly on the order of thousands of years (e.g., Hoang et al., 2010; Clift and Giosan, 2014), and the extent of human-disturbed drainage networks tends to be limited. Thus, published U–Pb ages of marine surface sediments near the river mouth (sample S2-5; Fig. 1c; Zhong et al., 2017) are useful as a reference of zircon contributions from the near-modern Pearl River and are compared in Fig. 7.

The main clusters of zircon crystallization ages do not vary much between the Lower and Upper Oligocene strata, mainly composed of Yanshanian ages and subordinately Indonesian and Caledonian ages as well as scattered Proterozoic ages (Fig. 7). While the recognizable spectra of three Phanerozoic groups, albeit with some minor changes in relative magnitudes and age peaks, continue stratigraphically upward, the average relative percentage of 500–3000-Ma ages feature an overall increasing trend, from 28.3% in Oligocene strata to 45.5% in Miocene strata to 51.7% in modern sediments. Moreover, the common Proterozoic age peak at ca. 950 Ma in both Lower Miocene strata and modern coastal sediments is nearly absent in Middle Miocene strata.

6. Discussion

6.1. Provenance interpretation and drainage evolution

The age signatures between Oligocene to present sediments from the northern Pearl River Mouth Basin and the earlier defined source areas (Figs. 6 and 7) are compared to investigate the detrital zircon provenance evolution of the region. A newly-developed, Monte Carlo-based sediment unmixing approach for detrital geochronological data (Sundell and Saylor, 2017) is also adopted here to quantify mixing proportions of potential sources (Fig. 8), which, compared to taxonomic categorizations like MDS analysis, is more powerful in conveying the possible drainage configuration. The desired mixing coefficients are obtained according to the best values computed from quantitative comparisons between observed and modeled zircon age distributions of sedimentary records. To avoid overreliance on any single goodness-of-fit

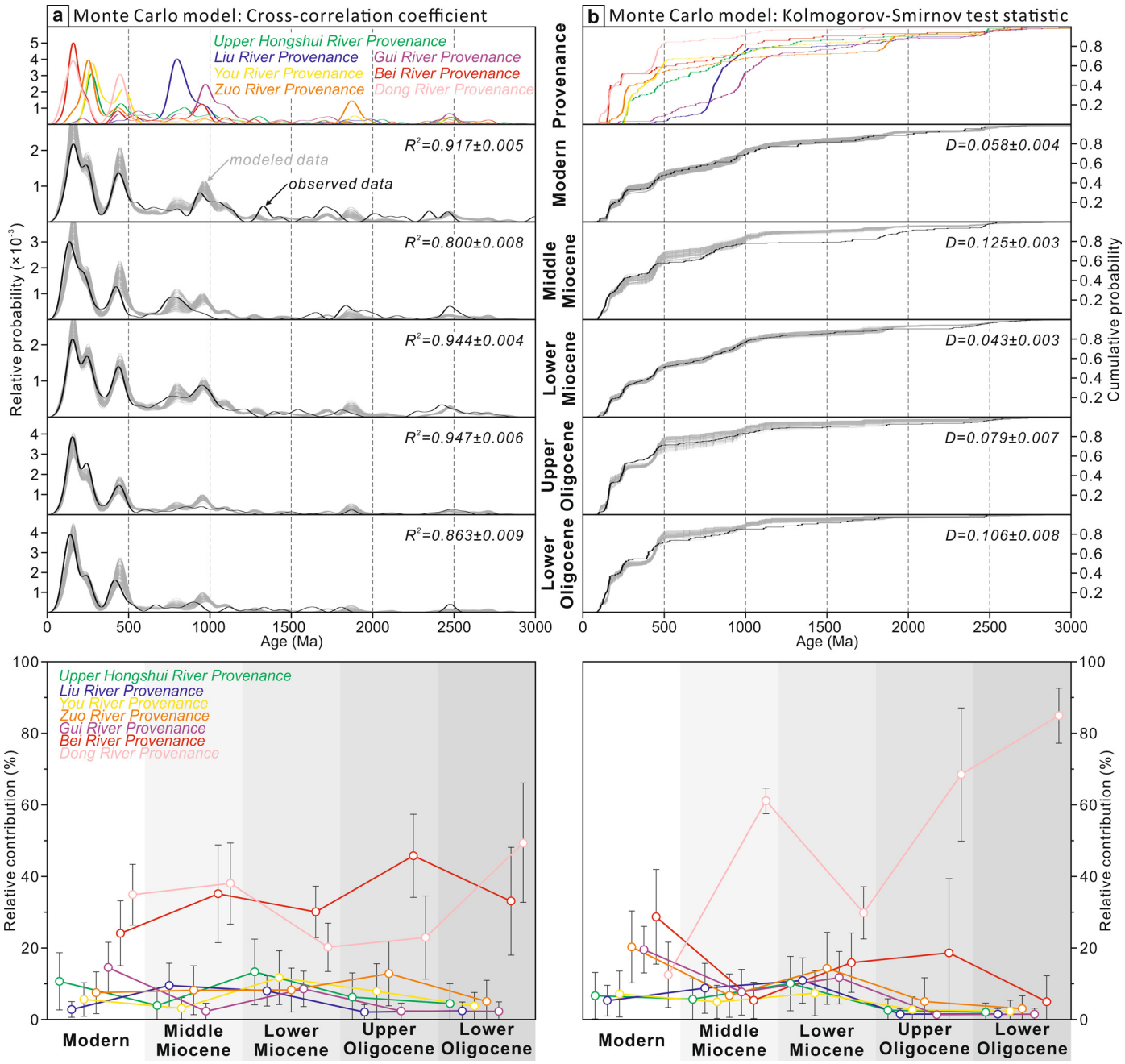

Fig. 8. Mixture combinations of defined potential provenances for the Oligocene–Middle Miocene Pearl River Mouth Basin and the modern river mouth, generated by the Monte Carlo unmixing model (Sundell and Saylor, 2017) using (a) the cross-correlation coefficient (R^2) plotted as kernel density estimation (KDE) spectra (bandwidth = 30 Ma) and (b) the Kolmogorov–Smirnov (K–S) test statistic (D) as cumulative distribution functions to assess best fits between observed and modeled data (10,000 trials). The obtained mean R^2 and D values range from 0.800–0.947 and 0.043–0.125, respectively, generally indicating a high degree of confidence. The mixing coefficients are reported at 1σ level of uncertainty (see Table S3 for details). (For interpretation of the colors in this figure, the reader is referred to the web version of this article.)

metric, both cross-correlation coefficient (R^2) and K–S test statistic (D) are implemented in the modeling. It should be noted that this unmixing approach still suffers from large external uncertainties likely induced by inappropriate choice of bandwidth for age frequency distributions, small sample size of particular age datasets, and poor characterization of source areas. Thus, the provenance interpretation and drainage evolution presented below are constrained not only by visual and model-based inspections of age data but also by geological plausibility.

6.1.1. Pre-Oligocene and Early Oligocene

During the Late Paleocene–Eocene, the South China margin underwent a prolonged period of widespread extension and continental rifting, forming several rift basins including the Pearl River Mouth Basin (Morley, 2016). The intensive faulting and episodic volcanism of the region would likely restrain the development of a continuous, large-scale river system. The Eocene syn-rift sediments sporadically drilled in the Pearl River Mouth Basin (Shao et al., 2016; Wang et al., 2017) and further south close to the continental–oceanic boundary (Liu et al., 2017; Shao et al., 2017) have been interpreted to be derived from the preexisting arc-related rocks of intrabasinal source terranes because of dominant Late Mesozoic ages of detrital zircons therein.

The fluvial provenance from the ancestral Pearl River was probably initiated as early as in the late Early Oligocene as suggested by a large set of southward-prograding deltaic sequences observed in

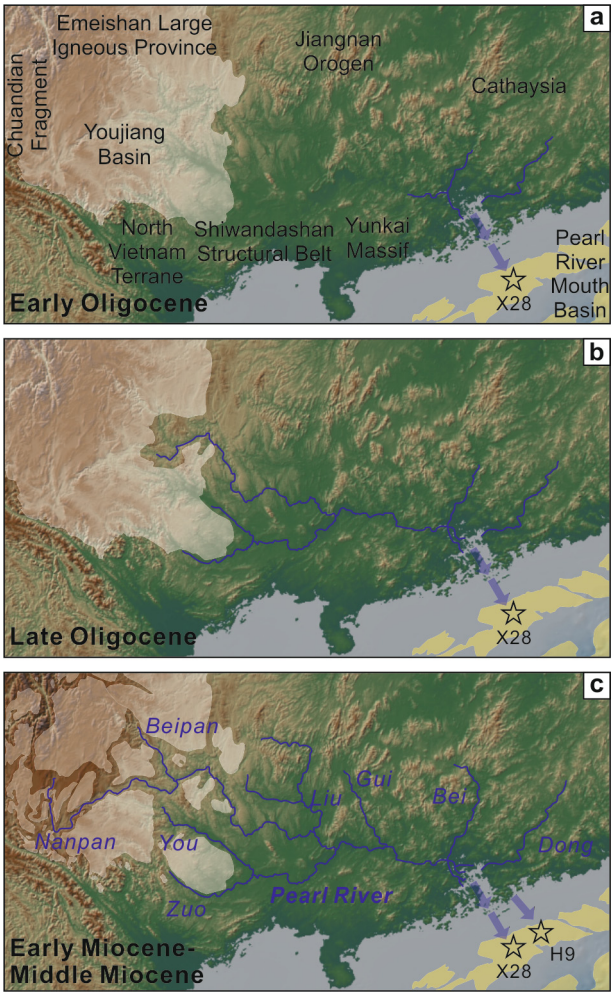

Fig. 9. Schematic reconstructions for the Oligocene–Middle Miocene drainage evolution of the Pearl River in response to the landscape evolution of the SE Tibetan Plateau, superimposed on the modern topographic map. (a) During the Early Oligocene, sediments in the northern Pearl River Mouth Basin (yellow shaded areas) were mainly sourced from small rivers (blue lines) draining eastern Cathaysia, as represented by arrows pointing from the river mouth to the studied borehole X28. Meanwhile, SE Tibet was likely dominated by a low-relief, high-elevation topography (white shaded areas). (b) While rivers in eastern Cathaysia continued to be the major provenances of the northern Pearl River Mouth Basin during the Late Oligocene, the western tributaries of the paleo-Pearl River were rapidly initiated by incision into the plateau margin and potentially supplied a growing amount of sediments eroded from inland South China. (c) By the Early Miocene, a near-modern drainage configuration of the paleo-Pearl River may have been established and the formerly continuous landscape in SE Tibet may have been significantly incised into a mosaic of low-relief, high-elevation surface patches. Note the provenance of the Middle Miocene strata in borehole H9 was different from that of the Lower Miocene strata in borehole X28 likely due to local contributions from eastern Cathaysia. (For interpretation of the colors in this figure, the reader is referred to the web version of this article.)

offshore seismic data (Pang et al., 2009) and well-rounded zircon shapes found in sample X28-2 (Shao et al., 2016). The most likely provenance of the Lower Oligocene strata is granite-dominated coastal South China (Fig. 9a; Shao et al., 2016) because the high percentage of Yanshanian zircons in association with the sporadic occurrence of Proterozoic zircons in sample X28-2 are exclusively found in Bei River Provenance and Dong River Provenance (Figs. 6 and 7). The Monte Carlo model results also show that a combination of the two provenances can explain the majority (average 82.5% and 89.8% for R^2-based and D-based models, respectively; Table S3) of zircon age distribution in the Lower Oligocene. As the zircon age signature of Bei River Provenance may overlap with that of Dong River Provenance (Fig. 6), a disparity in their individual contribution between two goodness-of-fit metrics is not unexpected (Fig. 8). By contrast, the average mixing proportions for other sources are generally less than 5% (Table S3), indicating that the drainage area of a paleo-Xi River, if existed, would likely be limited at that time (Fig. 9a).

6.1.2. Late Oligocene and Early Miocene

Although the overall age signatures between Upper Oligocene and Lower Oligocene strata appear visually similar (Fig. 7), two distinct mixture scenarios are indicated by the Monte Carlo modeling (Fig. 8). While in the D-based model the strongly dominant contributions from Bei River Provenance and Dong River Provenance continued through the Oligocene, the R^2-based model yields a small increase in relative contributions from Upper Hongshui River Provenance, You River Provenance, and Zuo River Provenance (Table S3). We favor the latter scenario because the Late Oligocene addition of provenances farther inland South China would supply more crustally evolved detritus eroded from Proterozoic–Lower Mesozoic bedrocks to the northern South China Sea, which is consistent with not only the conspicuous abundance of Proterozoic zircons found in sample X28-9 (Fig. S1) but also the onset of a negative Nd isotopic excursion observed in contemporary sediments from the Pearl River Mouth Basin (Shao et al., 2008) and ODP Site 1148 (Clift et al., 2002; Li et al., 2003). Although drainage networks connecting inland source terranes cannot be exactly determined, the generally low contributions from Upper Hongshui River Provenance (6.2 $\pm$ 6.8%) and You River Provenance (7.9 $\pm$ 7.7%) suggest that the paleo-Xi River probably originated from the eastern margin of the Youjiang Basin (Fig. 9b).

Along with the rift to post-rift transition of the northern South China Sea margin between Late Oligocene and Early Miocene times, the northern Pearl River Mouth Basin was dominated by a continental shelf to deltaic environment (Fig. 3; Zhao et al., 2009). The occurrence of a large percentage of Proterozoic zircons, especially those dated around 500–1000 Ma, in the Lower Miocene strata of borehole X28 (Fig. 7), when compared against the age signatures of potential sources (Fig. 6), suggests the possibility of a significant sediment supply from Upper Hongshui River Provenance, Liu River Provenance, and Gui River Provenance. The two modeled mixture scenarios are largely similar (Fig. 8), with the average individual contribution from a combination of Upper Hongshui River–Liu River–You River–Zuo River–Gui River provenances showing a range of from 8.2% to 13.3% in the R^2-based model and from 7.4% to 14.3% in the D-based model (Table S3). Moreover, despite different goodness-of-fit metrics implemented, a comparison of model results between Upper Oligocene and Lower Miocene strata consistently reveals a continuous rise in contributions from Upper Hongshui River Provenance and You River Provenance as well as a new addition of Liu River Provenance and Gui River Provenance. Thus, during the Early Miocene, the paleo-Xi River drainage basin had probably already expanded northward to the Jiangnan Orogen and westward towards the western Youjiang Basin (Fig. 9c). The total provenance contribution of extensively drained inland South China was of a similar level as that of coastal South China (Table S3).

6.1.3. Middle Miocene and present

The Monte Carlo model for the Middle Miocene strata of borehole H9 yields different mixture scenarios (Fig. 8; Table S3): in the R^2-based type the best-fit combination is mainly composed of Bei River Provenance (35.1 $\pm$ 13.7%) and Dong River Provenance (38.0 $\pm$ 11.4%) and subordinately Liu River Provenance (9.5 $\pm$ 6.2%) and Zuo River Provenance (8.2 $\pm$ 6.8%); in the D-based type the mixing proportion of Dong River Provenance (61.1 $\pm$ 3.6%) is much higher than that of the other provenances (average between 4.9% and 8.7%). Despite this difference, these model results, when compared to the case of Lower Miocene, consistently show a strongly en-

hanced Dong River Provenance and decreased contributions from Upper Hongshui River–You River–Gui River provenances (Table S3). An intuitive interpretation is a major drainage reorganization of the paleo-Pearl River occurring between Early and Middle Miocene; however, the dramatic loss of preexisting headwater drainage areas in the Youjiang Basin region would be in contradiction to the roughly unchanged εNd value observed within the Lower–Middle Miocene strata from the northern South China Sea (Li et al., 2003; Shao et al., 2008). Alternatively, this inter-stratal variation in zircon age signatures (Fig. 7) may represent a different spatial response to the paleo-Pearl River provenance. As borehole H9 is located closer to the eastern Cathaysia margin than borehole X28, a strong local influence of the Dong River Provenance would likely dilute relative source contributions from inland South China to the Middle Miocene Pearl River Mouth Basin (Fig. 9c).

The Monte Carlo model for modern coastal sediments near the river mouth yields a good fit with average R^2 and D values of 0.917 and 0.058, respectively (Fig. 8), but we caution against the geological reliability of modeled source contributions. In the R^2-based model, the negligible contribution from Liu River Provenance (2.8 $\pm$ 2.2%) and appreciable contribution from Gui River Provenance (14.5 $\pm$ 7.1%) (Table S3) seem incongruent with the fact that the current watershed area and average annual discharge of Gui River are about three times lower than those of Liu River (Fig. 1a). In the D-based model, the contribution from Zuo River Provenance (19.5 $\pm$ 6.5%) is abnormally high compared to those from Upper Hongshui River Provenance (6.6 $\pm$ 6.5%) and You River Provenance (7.1 $\pm$ 6.4%) (Table S3), which is apparently biased by the similarity of age distributions between coastal sample S2–5 and Zuo River samples 903 and R5 as shown in the MDS map (Fig. 5b). In addition, the model results tend to suffer from the very fine grain-size class of sample S2–5 (Zhong et al., 2017) where zircon is generally found in low concentrations and age data from insufficient zircon analyses are somewhat scattered (Fig. 7). Despite these misrepresentations, it is noteworthy for a visual comparison of compiled age data between Lower Miocene strata and modern coastal sediments that their KDE patterns are largely comparable, with common age clusters peaking at ca. 160 Ma, ca. 240 Ma, ca. 440 Ma, and ca. 950 Ma (Fig. 7). Thus, it is possible that the Pearl River has retained a near-modern configuration of drainage networks since the Early Miocene, and this interpretation is compatible with the previous Nd isotopic data (Clift et al., 2002; Shao et al., 2008).

6.2. Low-relief, high-elevation surface formation

6.2.1. Oligocene surface uplift

The provenance shift associated with drainage evolution between Late Oligocene and Early Miocene is explicitly manifested, visually in zircon age distribution patterns of KDEs and histograms, and numerically in unmixing models. Due to limited sampling space, this study lacks the ability to definitively estimate the variation tendency of zircon age signatures within each stratum. Nevertheless, previous densely sampled geochemical and Nd isotopic data from the northern South China Sea generally revealed a small-scale variability in provenance proxies within Lower Oligocene and Lower–Middle Miocene strata but a gradual, appreciable shift within Upper Oligocene strata (Li et al., 2003; Shao et al., 2008), pointing to the possibility that the westward expansion of the Pearl River drainage basin was a short-lived process that occurred in Late Oligocene time.

Although we should not ignore the role of climatic reorganization around the Oligocene–Miocene boundary in regulating individual provenance contributions, the Late Oligocene addition of inland provenances and the Cenozoic crustal thickening and growth of SE Tibet may be relevant in suggesting an underlying tectonic driver for the Pearl River drainage expansion. As the generation and propagation of topographic signals appear to predate or be coeval with the preservation of provenance signals in sedimentary records, the surface uplift of SE Tibet margin, according to our zircon provenance data, must have occurred as early as during the Late Oligocene. This minimum estimate, together with the Eocene near-sea-level paleoaltimetry reconstruction of SE Yunnan (Hoke et al., 2014), constrain the provenance shift-associated uplift initiation in SE Tibet margin to the Oligocene, which is consistent with the timing of drainage reorganization between Yangtze and Red rivers proposed by Clift et al. (2006) and Zheng et al. (2013). Coeval rapid exhumation has also been sporadically reported in thermochronometric studies conducted in this region (Wang et al., 2012; Shen et al., 2016; Wang et al., 2016). Whether these Oligocene topographic growth events are correlated as representing a regional-scale tectonic perturbation or are only locally generated is still uncertain, but it is becoming increasingly clear that the uplift of SE Tibet was not a single stage concentrated in Late Cenozoic as previously envisaged (e.g., Clark et al., 2005; Ouimet et al., 2010). The high topography of SE Tibet might already have been established during the Eocene, extending southeastward from central Tibet to as far as 25–26°N (e.g., Hoke et al., 2014; Li et al., 2015; Linnemann et al., 2017).

Apart from SE Tibet, our provenance data also record an addition of contributions from Liu River Provenance and Gui River Provenance between Late Oligocene and Early Miocene (Figs. 9b and 9c), which may be associated with a Cenozoic uplift and reactivation of the western Jiangnan Orogen.

6.2.2. Relict or in situ-generated low relief?

Based on the provenance interpretations of the Pearl River Mouth Basin presented above, the paleo-Pearl River drainage basin was initiated first in eastern Cathaysia during the Early Oligocene and then actively propagated towards the inland region of South China (Fig. 9). By the Early Miocene, the areas sandwiched between the upper Yangtze and Red Rivers in the SE Tibetan Plateau margin may have been extensively drained by the paleo-Pearl River, and this drainage pattern may continue into the Middle Miocene. The drainage expansion process is compatible with the relict landscape model and accordingly excludes the applicability of the model involving drainage area loss feedback during the time periods we investigated. Thus, before the rapid development of the paleo-Xi River between Late Oligocene and Early Miocene, a formerly continuous, if complex, low-relief landscape may already have existed in SE Tibet (Fig. 2a).

The functioning of the relict landscape model generally requires a regional relative base-level fall of drainage basins in SE Tibet. An intuitive explanation is that SE Tibet was a slowly eroding peneplain during the Early Cenozoic before being warped upward in the Middle–Late Cenozoic, e.g., by lower crustal flow away from central Tibet and SE Tibetan crust inflation (Clark et al., 2006; Ouimet et al., 2010). In this case, the Oligocene uplift initiation interpreted above may have directly triggered the relative base-level fall and rapid fluvial incision into a developing plateau margin. Alternatively, the elevated, high-relief mountain ranges formed by Oligocene crustal shortening and lateral extrusion were first beveled by an internal drainage smoothing process before a subsequent integration of external drainages (i.e., paleo-Xi River) across the plateau margin (Tapponnier et al., 2001; Liu-Zeng et al., 2008). However, this question of whether surface uplift or low-relief topography was produced first cannot be resolved by our present provenance data, and still requires high spatial and temporal resolution measurements of paleoaltimetric and thermochronometric records.

Unfortunately, the detrital zircon record of Upper Miocene–Pliocene strata in the Pearl River Mouth Basin is missing in our

study and the acquired age data from Middle Miocene strata tend to be biased by proximal provenance contributions, which renders the Late Cenozoic drainage evolution of the Pearl River subject to future research. As pointed out by Yang et al. (2015), a regional increase in uplift rate would be expected to accompany the shortening required for the initiation of drainage area loss feedback. Based on our current data, it is indeed possible that western tributaries of the Pearl River already dissected the westernmost Youjiang Basin or, farther inland, the Chuandian–Emeishan region during the Early–Middle Miocene (Fig. 2b) followed by a progressive contraction of headwater drainage basins during the Late Cenozoic, and if so, the area loss feedback model would still come into play. However, this possibility may be less likely because of the following considerations independent of the morphometric criteria of Whipple et al. (2017). First, the zircon age signature of modern coastal sediments is comparable to that of Lower Miocene strata from the Pearl River Mouth Basin (Fig. 7), rather than displaying an appreciable percentage decrease in Hercynian and Neoproterozoic age clusters that typically characterize the source terranes in SE Tibet (Fig. 6), indicating a near-modern configuration of drainage networks since the Early Miocene. Second, the prolonged, episodic surface uplift and river incision into the plateau margin, at least including an initial uplift during the Oligocene suggested by our provenance data and a regional-scale uplift during the Late Cenozoic suggested by previous thermochronometric data (Clark et al., 2005; Wang et al., 2012), tend to induce a progressive entrenchment of the already developed upper paleo-Xi River (Figs. 9b and 9c) into deep gorges, making a subsequent loss of these drainage areas by divide migration very difficult. Third, because of a nearly ten-fold difference in short- and long-term erosion rates on low-relief surfaces and in incised gorges of SE Tibet (Whipple et al., 2017), the migration of drainage divides driven by trunk-stream incision is expected to be substantially faster than the rate of lowering of hill slopes in the captured catchments. This potential inefficiency in relief reduction, and in view of the localized crustal deformation due to ongoing India–Asia convergence (Li et al., 2017) and the relatively short duration of potential area loss feedback during the Late Cenozoic, tends to restrain the frequency and magnitude of such in situ-produced topography. Fourth, in a regional context, if the Neogene drainage dynamics had played a dominant role in shaping the topography of SE Tibet, sedimentary archives from other large external fluvial systems would have recorded corresponding changes. The almost unchanged provenance signatures from lower reaches of both Yangtze River and Red River, however, suggest the continental-scale drainage systems connecting the Tibetan Plateau to the China seas have achieved a relatively stable configuration at least since the Miocene (e.g., Clift et al., 2006; Zheng et al., 2013).

7. Conclusions

Much current debate over the origin of low-relief, high-elevation landscapes in SE Tibet centers on the implementation and interpretation of morphometric analyses. This study aims to test the relevant formation mechanisms from a new provenance perspective by establishing causal relationships among provenance signature of the northern Pearl River Mouth Basin, drainage evolution of the Pearl River, and landscape change of inland South China.

Qualitative and quantitative comparisons of detrital zircon U–Pb age data between defined source terranes and Oligocene–Middle Miocene basin samples confirm a significant provenance shift event in response to drainage network expansion of the Pearl River. The northern and eastern tributaries of the ancestral Pearl River may be initiated first in eastern Cathaysia as early as in the Early Oligocene, followed by a progressive development of the western tributaries during the Late Oligocene. A near-modern drainage configuration may have been retained since the Early Miocene with the Liu and Gui rivers draining the Jiangnan Orogen and the Hongshui and Yu rivers draining the Youjiang Basin. It should be noted that this drainage reconstruction is only representative of zircon contribution, and its potential validity in other provenance metrics still requires additional restrictions on e.g., zircon fertility of source terranes and chemical and isotopic fractionations.

The provenance shifts well documented in the ocean basin along with the paleoaltimetry reconstructions sporadically conducted in SE Tibet constrain an Oligocene start of surface uplift in the plateau margin, earlier than the Late Cenozoic regional-scale exhumation as previously envisaged. Meanwhile, the Oligocene–Miocene drainage expansion process of the Pearl River indicates that the dominant formation mechanism of peculiar topography in SE Tibet likely involves the fluvial incision into a preexisting elevated, low-relief landscape, instead of the simultaneous in situ relief reduction and surface uplift in response to a self-sustained feedback from drainage area loss. Admittedly, this interpretation somewhat suffers from the problem of lack of zircon record of Upper Miocene–Pliocene strata, and still needs to be verified by future investigations of a more continuous and expanded sedimentary record. However, this paper highlights the value of provenance analysis in characterizing the low-relief, high-elevation surface formation, which can be readily applied to the regions other than SE Tibet.

Acknowledgements

We thank China National Offshore Oil Corporation (CNOOC) for providing geological data and borehole samples. We also thank Joel Saylor, Jing Liu-Zeng, and Shihu Li for commenting on an earlier version of this paper. Constructive reviews by two anonymous referees and editorial handling by An Yin are gratefully appreciated. This work was supported by National Natural Science Foundation of China (grant numbers 91128207 and 41576059) and National Science and Technology Major Project (grant number 2016ZX05026004-002). DJJvH was supported by NWO-VIDI grant 864.11.004. LC acknowledges the China Scholarship Council for supporting his visiting study at Utrecht University.

Appendix A. Supplementary material

Supplementary material related to this article can be found online at https://doi.org/10.1016/j.epsl.2018.05.039.

References

Allen, P.A., 2008. From landscapes into geological history. Nature 451, 274–276.
Andersen, T., 2002. Correction of common lead in U–Pb analyses that do not report ^{204}Pb. Chem. Geol. 192, 59–79.
Clark, M.K., House, M., Royden, L., Whipple, K., Burchfiel, B., Zhang, X., Tang, W., 2005. Late Cenozoic uplift of southeastern Tibet. Geology 33, 525–528.
Clark, M.K., Royden, L.H., 2000. Topographic ooze: building the eastern margin of Tibet by lower crustal flow. Geology 28, 703–706.
Clark, M.K., Royden, L.H., Whipple, K.X., Burchfiel, B.C., Zhang, X., Tang, W., 2006. Use of a regional, relict landscape to measure vertical deformation of the eastern Tibetan Plateau. J. Geophys. Res. 111, F03002.
Clift, P.D., Blusztajn, J., Nguyen, A.D., 2006. Large-scale drainage capture and surface uplift in eastern Tibet–SW China before 24 Ma inferred from sediments of the Hanoi Basin, Vietnam. Geophys. Res. Lett. 33, L19403.
Clift, P.D., Giosan, L., 2014. Sediment fluxes and buffering in the post-glacial Indus Basin. Basin Res. 26, 369–386.
Clift, P.D., Lee, J.I., Clark, M.K., Blusztajn, J., 2002. Erosional response of South China to arc rifting and monsoonal strengthening; a record from the South China Sea. Mar. Geol. 184, 207–226.
England, P., Molnar, P., 1990. Surface uplift, uplift of rocks, and exhumation of rocks. Geology 18, 1173–1177.
Hoang, L.V., Clift, P.D., Mark, D., Zheng, H., Tan, M.T., 2010. Ar–Ar muscovite dating as a constraint on sediment provenance and erosion processes in the Red and Yangtze River systems, SE Asia. Earth Planet. Sci. Lett. 295, 379–389.

Hoang, L.V., Wu, F., Clift, P.D., Wysocka, A., Swierczewska, A., 2009. Evaluating the evolution of the Red River system based on in situ U–Pb dating and Hf isotope analysis of zircons. Geochem. Geophys. Geosyst. 10, Q11008.

Hoke, G.D., Liu-Zeng, J., Hren, M.T., Wissink, G.K., Garzione, C.N., 2014. Stable isotopes reveal high southeast Tibetan Plateau margin since the Paleogene. Earth Planet. Sci. Lett. 394, 270–278.

Hu, D., Clift, P.D., Böning, P., Hannigan, R., Hillier, S., Blusztajn, J., Wan, S., Fuller, D.Q., 2013. Holocene evolution in weathering and erosion patterns in the Pearl River delta. Geochem. Geophys. Geosyst. 14, 2349–2368.

Lehrmann, D.J., Chaikin, D.H., Enos, P., Minzoni, M., Payne, J.L., Yu, M., Goers, A., Wood, T., Richter, P., Kelley, B.M., Li, X., Qin, Y., Liu, L., Lu, G., 2015. Patterns of basin fill in Triassic turbidites of the Nanpanjiang basin: implications for regional tectonics and impacts on carbonate-platform evolution. Basin Res. 27, 587–612.

Li, C.-F., Xu, X., Lin, J., Sun, Z., Zhu, J., Yao, Y., Zhao, X., Liu, Q., Kulhanek, D.K., Wang, J., Song, T., Zhao, J., Qiu, N., Guan, Y., Zhou, Z., Williams, T., Bao, R., Briais, A., Brown, E.A., Chen, Y., Clift, P.D., Colwell, F.S., Dadd, K.A., Ding, W., Almeida, I.H., Huang, X.-L., Hyun, S., Jiang, T., Koppers, A.A.P., Li, Q., Liu, C., Liu, Z., Nagai, R.H., Peleo-Alampay, A., Su, X., Tejada, M.L.G., Trinh, H.S., Yeh, Y.-C., Zhang, C., Zhang, F., Zhang, G.-L., 2014. Ages and magnetic structures of the South China Sea constrained by deep tow magnetic surveys and IODP Expedition 349. Geochem. Geophys. Geosyst. 15, 4958–4983.

Li, L., Garzione, C.N., 2017. Spatial distribution and controlling factors of stable isotopes in meteoric waters on the Tibetan Plateau: implications for paleoelevation reconstruction. Earth Planet. Sci. Lett. 460, 302–314.

Li, S., Advokaat, E.L., van Hinsbergen, D.J.J., Koymans, M., Deng, C., Zhu, R., 2017. Paleomagnetic constraints on the Mesozoic–Cenozoic paleolatitudinal and rotational history of Indochina and South China: review and updated kinematic reconstruction. Earth-Sci. Rev. 171, 58–77.

Li, S., Currie, B.S., Rowley, D.B., Ingalls, M., 2015. Cenozoic paleoaltimetry of the SE margin of the Tibetan Plateau: constraints on the tectonic evolution of the region. Earth Planet. Sci. Lett. 432, 415–424.

Li, X.-h., Wei, G., Shao, L., Liu, Y., Liang, X., Jian, Z., Sun, M., Wang, P., 2003. Geochemical and Nd isotopic variations in sediments of the South China Sea: a response to Cenozoic tectonism in SE Asia. Earth Planet. Sci. Lett. 211, 207–220.

Linnemann, U., Su, T., Kunzmann, L., Spicer, R.A., Ding, W.N., Spicer, T.E.V., Zieger, J., Hofmann, M., Moraweck, K., Gärtner, A., Gerdes, A., Marko, L., Zhang, S.T., Li, S.F., Tang, H., Huang, J., Mulch, A., Mosbrugger, V., Zhou, Z.K., 2017. New U–Pb dates show a Paleogene origin for the modern Asian biodiversity hot spots. Geology 46, 3–6.

Liu-Zeng, J., Tapponnier, P., Gaudemer, Y., Ding, L., 2008. Quantifying landscape differences across the Tibetan Plateau: implications for topographic relief evolution. J. Geophys. Res. 113, F04018.

Liu, C., Clift, P.D., Carter, A., Böning, P., Hu, Z., Sun, Z., Pahnke, K., 2017. Controls on modern erosion and the development of the Pearl River drainage in the late Paleogene. Mar. Geol. 394, 52–68.

Liu, Q.Y., van der Hilst, R.D., Li, Y., Yao, H.J., Chen, J.H., Guo, B., Qi, S.H., Wang, J., Huang, H., Li, S.C., 2014. Eastward expansion of the Tibetan Plateau by crustal flow and strain partitioning across faults. Nat. Geosci. 7, 361–365.

Liu, Y., Gao, S., Hu, Z., Gao, C., Zong, K., Wang, D., 2009. Continental and oceanic crust recycling-induced melt–peridotite interactions in the Trans-North China Orogen: U–Pb dating, Hf isotopes and trace elements in zircons from mantle xenoliths. J. Petrol. 51, 537–571.

Morley, C.K., 2016. Major unconformities/termination of extension events and associated surfaces in the South China seas: review and implications for tectonic development. J. Asian Earth Sci. 120, 62–86.

Ouimet, W., Whipple, K., Royden, L., Reiners, P., Hodges, K., Pringle, M., 2010. Regional incision of the eastern margin of the Tibetan Plateau. Lithosphere 2, 50–63.

Pang, X., Chen, C., Zhu, M., He, M., Shen, J., Lian, S., Wu, X., Shao, L., 2009. Baiyun movement: a significant tectonic event on Oligocene/Miocene boundary in the northern South China Sea and its regional implications. J. Earth Sci. 20, 49–56.

Robl, J., Hergarten, S., Prasicek, G., 2017. The topographic state of fluvially conditioned mountain ranges. Earth-Sci. Rev. 168, 190–217.

Saylor, J.E., Sundell, K.E., 2016. Quantifying comparison of large detrital geochronology data sets. Geosphere 12, 203–220.

Shao, L., Cao, L., Pang, X., Jiang, T., Qiao, P., Zhao, M., 2016. Detrital zircon provenance of the Paleogene syn-rift sediments in the northern South China Sea. Geochem. Geophys. Geosyst. 17, 255–269.

Shao, L., Meng, A., Li, Q., Qiao, P., Cui, Y., Cao, L., Chen, S., 2017. Detrital zircon ages and elemental characteristics of the Eocene sequence in IODP Hole U1435A: implications for rifting and environmental changes before the opening of the South China Sea. Mar. Geol. 394, 39–51.

Shao, L., Pang, X., Chen, C., Shi, H., Li, Q., Qiao, P., 2008. Late Oligocene sedimentary environments and provenance abrupt change event in the northern South China Sea. Front. Earth Sci. China 2, 138–146.

Shao, L., Qiao, P., Zhao, M., Li, Q., Wu, M., Pang, X., Zhang, H., 2015. Depositional characteristics of the northern South China Sea in response to the evolution of the Pearl River. Geol. Soc. (Lond.) Spec. Publ. 429, 31–44.

Shen, X., Tian, Y., Li, D., Qin, S., Vermeesch, P., Schwanethal, J., 2016. Oligocene–Early Miocene river incision near the first bend of the Yangze River: insights from apatite (U–Th–Sm)/He thermochronology. Tectonophysics 687, 223–231.

Sundell, K., Saylor, J.E., 2017. Unmixing detrital geochronology age distributions. Geochem. Geophys. Geosyst. 18, 2872–2886.

Tapponnier, P., Zhiqin, X., Roger, F., Meyer, B., Arnaud, N., Wittlinger, G., Jingsui, Y., 2001. Oblique stepwise rise and growth of the Tibet plateau. Science 294, 1671–1677.

Wang, C.-Y., Flesch, L.M., Silver, P.G., Chang, L.-J., Chan, W.W., 2008. Evidence for mechanically coupled lithosphere in central Asia and resulting implications. Geology 36, 363–366.

Wang, E., Kirby, E., Furlong, K.P., van Soest, M., Xu, G., Shi, X., Kamp, P.J.J., Hodges, K.V., 2012. Two-phase growth of high topography in eastern Tibet during the Cenozoic. Nat. Geosci. 5, 640–645.

Wang, W., Ye, J., Bidgoli, T., Yang, X., Shi, H., Shu, Y., 2017. Using detrital zircon geochronology to constrain Paleogene provenance and its relationship to rifting in the Zhu 1 Depression, Pearl River Mouth Basin, South China Sea. Geochem. Geophys. Geosyst. 18, 3976–3999.

Wang, Y., Zhang, B., Schoenbohm, L.M., Zhang, J., Zhou, R., Hou, J., Ai, S., 2016. Late Cenozoic tectonic evolution of the Ailao Shan–Red River fault (SE Tibet): implications for kinematic change during plateau growth. Tectonics 35, 1969–1988.

Whipple, K.X., DiBiase, R.A., Ouimet, W.B., Forte, A.M., 2017. Preservation or piracy: diagnosing low-relief, high-elevation surface formation mechanisms. Geology 45, 91–94.

Willett, S.D., McCoy, S.W., Perron, J.T., Goren, L., Chen, C.Y., 2014. Dynamic reorganization of river basins. Science 343, 1248765.

Wissink, G.K., Hoke, G.D., Garzione, C.N., Liu-Zeng, J., 2016. Temporal and spatial patterns of sediment routing across the southeast margin of the Tibetan Plateau: insights from detrital zircon. Tectonics 35, 2538–2563.

Yang, J., Cawood, P.A., Du, Y., Huang, H., Hu, L., 2014. A sedimentary archive of tectonic switching from Emeishan Plume to Indosinian orogenic sources in SW China. J. Geol. Soc. (Lond.) 171, 269–280.

Yang, R., Willett, S.D., Goren, L., 2015. In situ low-relief landscape formation as a result of river network disruption. Nature 520, 526–529.

Yin, A., Harrison, T.M., 2000. Geologic evolution of the Himalayan–Tibetan Orogen. Annu. Rev. Earth Planet. Sci. 28, 211–280.

Zhao, Z., Zhou, D., Liao, J., 2009. Tertiary paleogeography and depositional evolution in the Pearl River Mouth Basin of the northern South China Sea. J. Trop. Oceanogr. 28, 52–60 (in Chinese with English abstract).

Zheng, H., Clift, P.D., Wang, P., Tada, R., Jia, J., Hee, M., Jourdanf, F., 2013. Pre-Miocene birth of the Yangtze River. Proc. Natl. Acad. Sci. USA 110, 7556–7561.

Zhong, L., Li, G., Yan, W., Xia, B., Feng, Y., Miao, L., Zhao, J., 2017. Using zircon U–Pb ages to constrain the provenance and transport of heavy minerals within the northwestern shelf of the South China Sea. J. Asian Earth Sci. 134, 176–190.